

# Forbidden Dark Matter Combusted Around Supermassive Black Hole

Yu Cheng,<sup>1,2,\*</sup> Shao-Feng Ge,<sup>1,2,†</sup> Xiao-Gang He,<sup>1,2,3,‡</sup> and Jie Sheng<sup>1,2,§</sup>

<sup>1</sup>*Tsung-Dao Lee Institute & School of Physics and Astronomy, Shanghai Jiao Tong University, China*

<sup>2</sup>*Key Laboratory for Particle Astrophysics and Cosmology (MOE)*

*& Shanghai Key Laboratory for Particle Physics and Cosmology,  
Shanghai Jiao Tong University, Shanghai 200240, China*

<sup>3</sup>*Department of Physics, National Taiwan University, Taipei 10617, Taiwan*

The forbidden dark matter cannot annihilate into a pair of heavier partners, either SM particles or its partners in the dark sector, at the late stage of cosmological evolution by definition. We point out the possibility of reactivating the forbidden annihilation channel around supermassive black holes. Being attracted towards a black hole, the forbidden dark matter is significantly accelerated to overcome the annihilation threshold. The subsequent decay of the annihilation products to photon leaves a unique signal around the black hole, which can serve as a smoking gun for the forbidden dark matter. For illustration, the Fermi-LAT data around Sgr A\* provides a preliminary constraint on the thermally averaged cross section of the reactivated forbidden annihilation that is consistent with the DM relic density requirement.

**Introduction** – More than 80% of the matter in our Universe today are dark matter (DM) [1]. But the nature of DM is still a mystery and suggests new physics beyond the Standard Model (SM) of particle physics [2]. Various mechanisms of DM production in the early Universe have been proposed. The most classical one is the thermal freeze-out [3], especially for Weakly Interacting Massive Particle (WIMP). In this scenario, DM with weak scale mass and interacting strength can naturally predict the observed relic density, which is called the WIMP Miracle. There are also many other proposed DM production mechanisms to achieve the right relic density [4–22]. Of particular interest is the forbidden DM.

It was first noticed in [23] that the forbidden annihilation, where DM annihilates into heavier particles, can happen due to the high-energy tail of the thermalized velocity distribution in the early Universe. With heavier annihilation product, the forbidden channel is exponentially suppressed. This allows forbidden DM to have a stronger interaction strength than the usual  $\langle\sigma v\rangle \propto m_\chi$  scaling behavior of the WIMP freeze-out scenario. A typical realistic model introduces a heavy dark photon as a partner of the forbidden DM [24]. In addition to the forbidden channel that determines the relic abundance, this model also naturally introduces DM self-interaction. With tiny mass splitting, either positive or negative, this forbidden scenario has a variation as impeded DM [25]. More concrete models can be found in [26–28], in addition to an interesting  $3 \rightarrow 2$  channel [29].

However, the DM Boltzmann distribution with typically  $\mathcal{O}(100)$  km/s velocity dispersion in our galaxy nowadays can no longer support the forbidden channel. Although it is possible to create other annihilation channels into  $e^+e^-$  [24],  $\gamma\gamma$  [30–32], and other heavier particles [31, 32], they are suppressed by kinematic mixing or loop factor. The forbidden DM has a difficulty of being probed via indirect detection. One of the three major probes (direct, indirect, and collider detections) of DM

is almost completely missing. Then it becomes very hard to verify whether the DM, if found, is a forbidden type or not. It is of great importance to find a way of testing the forbidden nature of such scenario.

Around the supermassive black hole (SMBH), DM accretes and forms a spike due to the strong gravitational potential. This enhances the DM annihilation signals at the galaxy center (GC) [33–43]. Meanwhile, the velocity of DM keeps increasing along its way towards the SMBH [44, 45]. Comparison with the observed  $\gamma$ -ray flux from GC can put a constraint on the DM annihilation cross section [46–49]. However, the forbidden annihilation has not been discussed yet.

We point out for the first time that SMBH is a perfect place for testing the forbidden DM scenario. The SMBH acts as a natural particle accelerator and reactivates the forbidden annihilation into heavier particles. With further decay into photons, the DM spike then becomes a point source of  $\gamma$ -ray. We compare the predicted  $\gamma$ -ray spectrum with the Fermi-LAT observation for the emission around Sgr A\* in our galaxy center to constrain the forbidden annihilation cross section.

## Reactivating Forbidden Channel around SMBH

– For illustration, we adopt an economic scenario of forbidden DM with one DM particle  $\chi$ , one heavy partner  $F$ , and a light vector mediator  $\phi_\mu$ ,

$$\mathcal{L}_{\text{DM}} = g_\chi \phi \bar{\chi} \gamma^\mu \chi \phi_\mu + g_F \phi \bar{F} \gamma^\mu F \phi_\mu. \quad (1)$$

The annihilation channel  $\chi\bar{\chi} \rightarrow F\bar{F}$  is forbidden if DM  $\chi$  is lighter than the final-state  $F$ ,  $m_\chi \lesssim m_F$ . Typically, the DM velocity in galaxy is  $10^{-3}$  of the speed of light as determined by the galaxy gravitational potential. Correspondingly, the DM kinetic energy is only  $10^{-6}$  of its mass. A relative mass difference  $\Delta_{F\chi} \equiv (m_F - m_\chi)/m_\chi$  slightly larger than  $10^{-6}$  can forbid DM annihilation and the consequent indirect detection.

To reopen the forbidden channel, it is necessary to accelerate the DM particles to overcome the annihilation

threshold. This naturally happens when DM gets accreted around black hole, especially SMBH in the galaxy center. A DM particle can be easily accelerated to become relativistic. Especially, its velocity can reach the speed of light around the event horizon [45, 50]. With the help of a SMBH, forbidden DM can in principle overcome the annihilation threshold no matter how large the mass difference can be.

In its vicinity, the SMBH dominates gravitational potential. Considering a DM particle attracted from infinity, its velocity at distance  $r$  from the SMBH scales as  $v(r) \propto r^{-1/2}$ . Below we will give concrete evaluation of the DM density and velocity profiles in detail.

With self-scattering, the DM velocity and density profiles have more sophisticated dependence on the radius  $r$ . We divide the whole galaxy into three regions,

$$\rho(r) = \begin{cases} \text{Halo: } \rho_{\text{NFW}}(r), & r > r_1, \\ \text{Core: } \rho_{\text{iso}}(r), & r_0 < r < r_1, \\ \text{Spike: } \rho_{\text{spike}}(r), & r_{\text{in}} < r < r_0, \end{cases} \quad (2)$$

as shown in Fig. 1. The division  $r_1$  is the characteristic radius where the DM particle can experience one scattering on average during the halo age  $t_{\text{age}}$  [55]. For  $r > r_1$ , the DM is treated as collisionless and the Navarro-Frenk-White (NFW) profile [56],  $\rho(r) = \rho_s(r/r_s)^{-1}(1+r/r_s)^{-2}$  with  $\rho_s = 4.1 \times 10^6 M_\odot/\text{kpc}^3$  and  $r_s = 26 \text{ kpc}$  [49, 57], is a good approximation.

**Core:** For the inner region,  $r < r_1$ , DM experiences frequent collisions to maintain an isothermal core. Its DM density profile is obtained by solving the Jeans equation [55, 58]. On the boundary between the core and halo regions, the density is the same as the NFW profile to make the transition continuous. Since the NFW profile in the halo region is kept as the original one, the mass enclosed within  $r_1$  for the isothermal solution should also remain the same as its NFW counterpart. In other words, the NFW profile sets an initial condition for the core region. At the center, the isothermal DM profile approaches a constant density. With these conditions, the DM density  $\rho_0 \equiv \rho(r=0)$  and the one-dimensional velocity dispersion  $v_0$  of the isothermal core can be determined. In the current study, we take the transverse self-scattering cross section [59–62] to be  $\langle \sigma_T v \rangle / m_\chi = 1.5 (\text{cm}^2/\text{g}) \times (\text{km/s})$  for illustration. With a simple scaling  $\sigma_T \propto g_{\chi\phi}^4 / m_\chi^2$ , the coupling  $g_{\chi\phi}$  increases with the DM mass  $m_\chi$ ,  $g_{\chi\phi} \propto m_\chi^{3/4}$ . However, the coupling remains perturbative ( $g_{\chi\phi} < 1$ ) in the whole range under consideration. For the best-fit  $m_\chi = 6.6 \text{ GeV}$  from fitting the Fermi-LAT data as we elaborate later, the corresponding self-interaction coupling is  $g_{\chi\phi} = 0.021$ . With 10 Gyr galaxy age, the division between the halo and core regions happens at  $r_1 = 0.33 \text{ kpc}$ . The gravitational potentials of both baryons and dark matter are taken into consideration [58]. Then solving the Jeans equation gives a velocity dispersion  $v_0 = 99 \text{ km/s}$  and

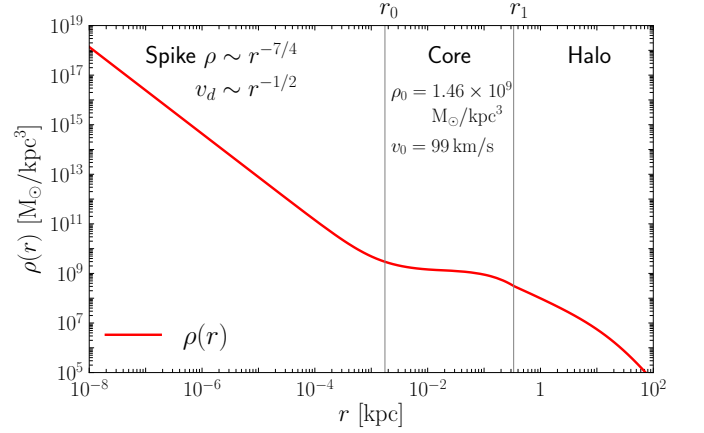


FIG. 1: The DM density profile  $\rho(r)$  as a function of radius  $r$ . The grey vertical lines divide the whole range into three regions: halo, core, and spike.

density  $\rho_0 = 1.46 \times 10^9 M_\odot/\text{kpc}^3$  inside the core region.

**Spike:** The DM core appears as a platform in the density profile. However, the influence of SMBH leads to a DM spike in the innermost region since the DM gas can no longer maintain isothermal in such a strong and deep gravitational potential. For  $r < r_0 \equiv GM/v_0^2$ , the gravitational force of SMBH dominates. The DM density matches with the core profile at  $r_0$ . Namely, the core profile provides an initial condition for the spike region. The density profile  $\rho(r)$  and the one-dimensional velocity dispersion  $v_d(r)$  inside the spike can then be obtained by numerically solving the coupled differential equations Eq.(33) and Eq.(34) of [63]. The exact solution follows power-law scaling in the majority part of the spike,  $\rho \propto r^{-(3+a)/4}$  and  $v_d(r) \propto r^{-1/2}$ . While the velocity scaling behavior is consistent with our naive expectation earlier and hence can apply universally, the density scaling is related to the velocity dependence of the self-scattering cross section  $\sigma = \sigma_0(v_d/v_0)^a$  via  $a$ . For illustration, a light mediator  $\phi$  with mass  $m_\phi \sim 10^{-3} m_\chi$  predicts  $a = 4$  and correspondingly  $\rho \propto r^{-7/4}$ . Fig. 1 shows our numerical evaluation of the spike DM density profile including relativistic effects. However, the DM density cannot increase forever towards the SMBH. It has a sharp cutoff and vanishes at an inner boundary  $r_{\text{in}} \equiv 4GM$  [63, 64].

From the core platform to the vicinity around SMBH, the DM density increases by at least 9 orders as shown in Fig. 1. Correspondingly, the DM self-scattering rate scales as  $\rho^2(r)$  and increases by at least 18 orders. So the DM fluid around SMBH is fully thermalized. Being relativistic, the DM velocity follows the Jüttner distribution [51, 52],

$$f_J(\mathbf{p}) = \frac{1}{4\pi T_\chi m_\chi^2 K_2(x)} e^{-\frac{\sqrt{|\mathbf{p}|^2 + m_\chi^2}}{T_\chi}}, \quad (3)$$

where the temperature parameter  $x \equiv m_\chi/T_\chi$  is the ratio of DM mass  $m_\chi$  and temperature  $T_\chi$ . The DM temperature is equivalent to its velocity dispersion,  $T_\chi = \frac{3}{2}m_\chi v_d^2$ . With  $v_d(r) \propto r^{-1/2}$ , the DM temperature ( $T_\chi \propto 1/r$ ) keeps increasing towards the SMBH to overcome the forbidden annihilation threshold.

**The Forbidden DM Signature** – With the forbidden channel  $\chi\bar{\chi} \rightarrow F\bar{F}$  being reactivated, the final-state  $F$  further decays into neutrino and photon ( $F \rightarrow \nu\gamma$ ) through the operator  $g_{F\nu A}\bar{F}\sigma^{\mu\nu}\nu\mathcal{F}_{\mu\nu}$  where  $\mathcal{F}_{\mu\nu}$  is the photon field strength. The photon can be collected by astrophysical  $\gamma$ -ray observations at Fermi-LAT. In principle, the DM particle  $\chi$  can also annihilate into a pair of mediators,  $\chi\bar{\chi} \rightarrow \phi\phi$ . At first glance, the light mediator can form ladder diagrams to enhance the annihilation cross section by the Sommerfeld enhancement [65–68]. However, this enhancement only happens with non-relativistic DM,  $v^2 \leq \alpha_d m_\phi/m_\chi$  with  $\alpha_d \equiv g_{\chi\phi}^2/(4\pi)$ , and hence does not apply here. In addition, this channel has no observable signal as will be detailed later. Unless stated otherwise, we focus on the forbidden channel  $\chi\bar{\chi} \rightarrow F\bar{F}$ .

With DM particles being fully thermalized and following the Juttner distribution in Eq. (3), the kinematics of a DM pair with momenta  $p_1$  and  $p_2$  can be parameterized in terms of the total invariant mass squared  $s \equiv (p_1 + p_2)^2$  or equivalently the relative velocity  $V_r$ , the centre-of-mass velocity  $V_c$  or equivalently the energy sum  $E_+ \equiv E_1 + E_2$ , and their energy difference  $E_- \equiv E_1 - E_2$ . The other three degrees of freedom in  $\mathbf{p}_1$  and  $\mathbf{p}_2$  can be reduced by symmetry considerations: 1) the overall two directional angles of  $\mathbf{p}_1 + \mathbf{p}_2$  by the spherical invariance of the whole system, and 2) another azimuthal angle by the rotational invariance around the total moment.

It is more convenient to first calculate the differential cross section in the center-of-mass frame where both the initial  $\chi$  and the final  $F$  have fixed energy,  $\sqrt{s}/2$ . For the  $s$ -channel annihilation dictated by Eq. (1),

$$\frac{d\sigma}{d\Omega} = g_{\chi\phi}^2 g_{F\phi}^2 \sqrt{\frac{s_F}{s_\chi}} \frac{s(4m_F^2 + 4m_\chi^2 + s) + \cos^2\theta_F^c s_F s_\chi}{64\pi^2 s(s - m_\phi^2)^2}, \quad (4)$$

with  $s_F \equiv s - 4m_F^2$  and  $s_\chi \equiv s - 4m_\chi^2$ . The angular dependence part  $\cos\theta_F^c$ , where  $\theta_F^c$  is the scattering angle between the  $F$  and total momenta, is highly suppressed by  $s_F$  and  $s_\chi$ . For  $m_\chi = 10$  GeV,  $m_F = 11$  GeV, and a typical  $s = 1.3 \times 4m_F^2$ , the angular dependent part only contributes 2%. For simplicity, we treat this process as isotropic.

The produced  $F$  further decays into photons with fixed energy  $m_F/2$  in the  $F$  rest frame. Lorentz boost back to the center-of-mass frame renders a box-shaped spectrum [69, 70],  $dN_\gamma/dE_\gamma = 1/(E_+^c - E_-^c)$  where limits  $E_\pm^c \equiv m_F\gamma_F(1 \pm v_F)/2$  with  $\gamma_F \equiv 1/\sqrt{1 - v_F^2}$  and  $v_F \equiv \sqrt{1 - 4m_F^2/s}$ . Since the primary process  $\chi\bar{\chi} \rightarrow F\bar{F}$  is isotropic in the center-of-mass frame, the box-shaped

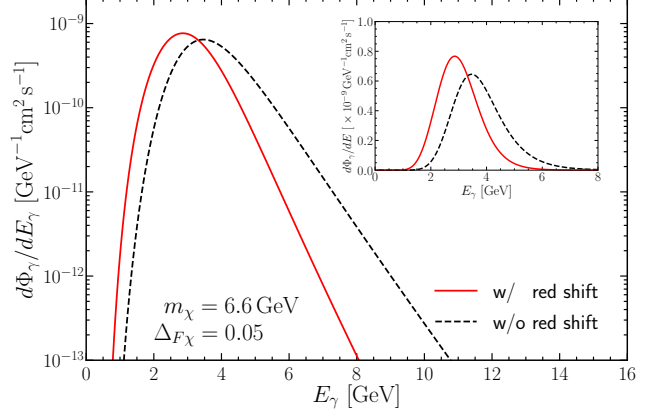


FIG. 2: The  $\gamma$ -ray spectrum  $d\Phi_\gamma/dE_\gamma$  illustrated with DM mass  $m_\chi = 6.6$  GeV and the relative mass difference  $\Delta_{F\chi} = 0.05$ . Correspondingly, the total flux injected is  $1.4 \times 10^{-9}$  cm<sup>2</sup>/s which is the best-fit value of the Fermi-LAT data. Both results with or without redshift are shown as red solid and black dashed lines, respectively. The insert plot shows the same results in linear scale.

photon spectrum is also isotropic.

It is necessary to further Lorentz boost to the lab frame where the photon spectrum is observed. Due to isotropy, photon of any given energy  $E_\gamma$  in the center-of-mass frame again possesses box-shaped spectrum in the lab frame,  $dN_\gamma/dE_\gamma = 1/(E_+^L - E_-^L)$  with limits  $E_\pm^L \equiv E_\gamma\gamma_c(1 \pm v_c)$ . The final photon spectrum in the lab frame is then a convolution of these two-step box spectra.

Since the two initial DM particles are fully thermalized, thermal average is necessary to obtain the photon spectrum,

$$\frac{dF_\gamma}{dE_\gamma}(r) = \int_0^1 dV_r dV_c P_r(V_r, V_c, x) \sigma V_r \frac{dN_\gamma}{dE_\gamma}(V_r, V_c). \quad (5)$$

For evaluating the total flux from DM annihilation, one needs to integrate over the radius  $r$ . However, not all DM particles can overcome the annihilation threshold. At a large radius, only the high-energy tail of the Juttner distribution can contribute. So there is no need to integrate the radius  $r$  to infinity. We may set an upper limit  $r_b$  on the radius integration. The concrete value of  $r_b$  can be numerically solved by requiring the local phase space to have at least 1% contribution above the annihilation threshold,

$$\int_0^{V_r^{\text{th}}} dV_r \int_0^1 dV_c P_r(V_r, V_c, x(r_b)) \equiv 0.99, \quad (6)$$

where  $V_r^{\text{th}} \equiv [1 - 1/(1 - 2m_F^2/m_\chi^2)^2]^{1/2}$  is the relative velocity at threshold. Note that the temperature parameter  $x(r)$ , as defined below Eq. (3), is a function of the radius since  $T_\chi$  is a function of  $r$ . The joint probability

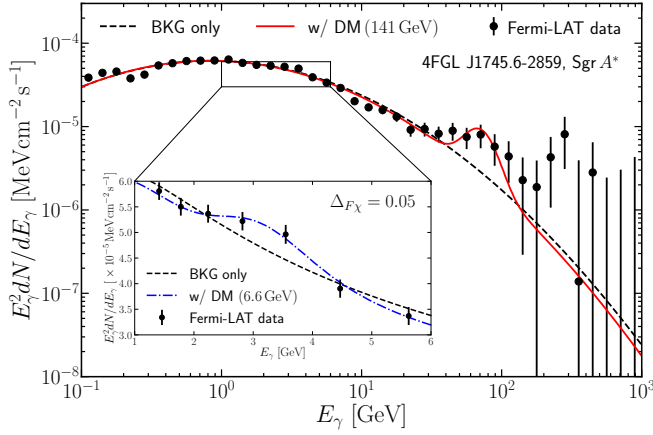


FIG. 3: The Fermi-LAT data (black points with error bar), background-only fit (black dashed line), and the signal fit with forbidden DM annihilation for  $m_\chi = 141$  GeV (red solid) and  $m_\chi = 6.6$  GeV (blue dash-dotted). For illustration, the mass difference between DM and its partner is taken to be  $\Delta_{F\chi} = 0.05$ .

distribution,

$$P_r(V_r, V_c, x) \equiv \frac{x^2}{K_2^2(x)} \frac{\gamma_r^3(\gamma_r^2 - 1)V_c^2}{(1 - V_c^2)^2} e^{-x\sqrt{\frac{2+2\gamma_r}{1-V_c^2}}}, \quad (7)$$

reduced from the two DM Jüttner distributions with momenta  $p_1$  and  $p_2$ , is a function of their relative velocity  $V_r \equiv \sqrt{\gamma_r^2 - 1}/\gamma_r$  ( $\gamma_r \equiv (p_1 \cdot p_2)/m_\chi^2$ ) and center-of-mass velocity  $V_c \equiv \sqrt{1 - s/(E_1 + E_2)^2}$  [53, 54]. For those regions with  $r > r_b$  and hence less than 1% of the total phase space that can contribute, we omit their contributions for simplicity which is a good enough approximation. While the integration volume increases as  $r^3$ , the DM mass density factor  $\rho^2(r) \sim r^{-7/2}$  decreases even faster as we demonstrate below. Consequently, the actual precision should be better than 1%.

The photon flux observed at Earth is then an integration,

$$\frac{d\Phi_\gamma}{dE_\gamma} = \frac{1}{4\pi D^2} \frac{1}{4m_\chi^2} \int_{r_{in}}^{r_b} 4\pi r^2 dr \rho^2(r) \frac{dF_\gamma}{dE_\gamma}(r), \quad (8)$$

with dilution by the distance  $D$  to the SMBH.

Due to the extremely strong gravitational potential around the SMBH, the emitted photon will lose energy when traveling towards us. This gravitational redshift reduces the photon energy by a factor of  $\sqrt{1 - 2GM/r_e}$  as a function of the radius  $r_e$  where the photon emitted. Fig. 2 shows the photon fluxes in Eq. (8) with (red solid) and without (black dashed) redshift. As expected, redshift drives the flux toward lower energy with a narrower width. It is interesting to see that the signal is actually a peak. Such a prominent feature can help itself to be identified in observations as we elaborate below.

**Constraints from FermiLAT** – The predicted photon flux is localized around the SMBH. We use the Fermi-LAT data to illustrate its constraint on the Forbidden DM. Being an all-sky  $\gamma$ -ray telescope, Fermi-LAT has very good energy and angular resolutions on the  $\gamma$ -ray point source from the GC [71, 72]. We analyze a total region of  $10^\circ \times 10^\circ$  square centered around the direction of Sgr A\* and find several  $\gamma$ -ray point sources, of which 4FGL J1745.6-2859 is the brightest and closest one to Sgr A\* in the Fourth catalog of Fermi-LAT sources (4FGL) [73, 74]. Also, this point source is considered as the manifestation of Sgr A\* in the MeV-to-GeV range [75]. We use 14 years of Fermi-LAT data from August 4, 2008 to October 26, 2022. To be specific, the Pass 8 SOURCE-class events from 100 MeV to 1000 GeV are binned to a pixel size of  $0.08^\circ$ .

A universal model can describe the  $\gamma$ -ray spectrum of different point sources. The 4FGL J1745.6-2859 spectral model is a log-parabola in the 4FGL Catalog [73, 74],

$$\frac{dN}{dE} = N_0 \left( \frac{E}{E_0} \right)^{-\alpha - \beta \log(E/E_0)}, \quad (9)$$

where  $N_0$  is normalization,  $E_0$  a scale parameter,  $\alpha$  the spectral slope at  $E_0$ , and  $\beta$  the curvature of the spectrum. Since  $E_0$  does not vary much, its value is fixed to 4074 MeV in our fit while the other three can freely adjust. Fig. 3 shows the observed data of energy spectrum from Fermi-LAT and the best-fit line using the universal model. The black dashed line shows that the background-only hypothesis can fit the data pretty well with  $\chi_{\min}^2 = 140.8$ .

The strength of the forbidden channel can be parametrized in terms of the *weighted thermally averaged cross section*  $\langle \sigma v \rangle$ ,

$$\langle \sigma v \rangle \equiv \frac{\int_{4GM}^{r_b} 4\pi r^2 \rho^2(r) \langle \sigma v(r) \rangle}{\int_{4GM}^{r_b} 4\pi r^2 \rho^2(r)}, \quad (10)$$

by taking the DM density  $\rho(r)$  and geometrical measure into consideration. Using  $\chi^2$  minimization, we find two local best-fit points at  $m_\chi = 6.6$  GeV and  $\langle \sigma v \rangle = 2.56 \times 10^{-25} \text{ cm}^3 \text{ s}^{-1}$  as well as  $m_\chi = 141$  GeV and  $\langle \sigma v \rangle = 5.32 \times 10^{-24} \text{ cm}^3 \text{ s}^{-1}$ . For the global fit point at  $m_\chi = 6.6$  GeV, the coupling constants are  $g_{\chi\phi} = 0.021$  and  $g_{F\phi} = 1.01$ . Compared with the background-only hypothesis,  $\chi_{\min}^2$  decreases by 17.0 and 14.2, respectively. Fig. 3 shows the best-fit energy spectrum with DM hypothesis as blue dash-dotted and red solid lines. We can clearly see the prominent bump around  $E_\gamma \approx 3$  GeV which corresponds to the  $m_\chi = 6.6$  GeV best-fit value. Although the  $E_\gamma = 60$  GeV peak in the observed spectrum seems more prominent in Fig. 3, it actually has lower significance due to larger uncertainty.

Fig. 4 shows the signal sensitivities obtained with  $\Delta_{F\chi} = 0.05$  and self-scattering cross section  $\langle \sigma_{TV} \rangle / m_\chi =$



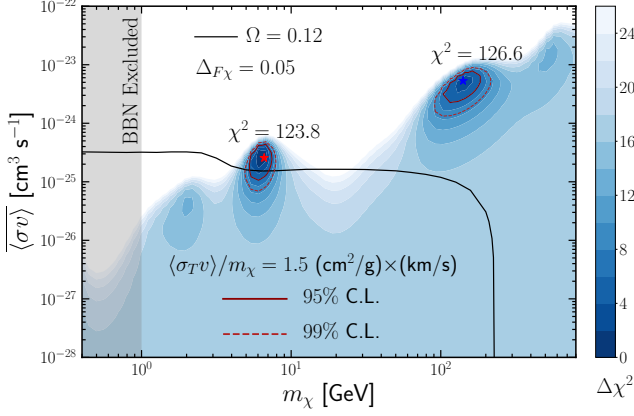


FIG. 4: The sensitivity contours of forbidden DM annihilation cross section obtained by fitting the Fermi-LAT data with mass difference  $\Delta_{F\chi} = 0.05$ ,  $m_\phi = 10^{-3}m_\chi$ , and self-scattering cross section  $\langle\sigma_T v\rangle/m_\chi = 1.5 (\text{cm}^2/\text{g}) \times (\text{km/s})$ . The red star represents the best-fit point where  $m_\chi = 6.6 \text{ GeV}$  and  $\langle\sigma v\rangle = 2.56 \times 10^{-25} \text{ cm}^3 \text{ s}^{-1}$ . The red solid and dashed lines are the sensitivity contours at 95% and 99% C.L., respectively. The black solid line corresponds to the parameters that generate the correct relic density  $\Omega_{\text{CDM}} = 0.12$  through freeze-out.

$1.5 \text{ cm}^2/\text{g} \times \text{km/s}$ . The sensitivity around the best-fit point with  $m_\chi = 6.6 \text{ GeV}$  is quite significant. We show the 95% (red solid) and 99% (red dashed) contours to make it transparent. With a peak structure in the inset of Fig. 2, the forbidden DM scenario can nicely explain the local excess around  $E_\gamma \approx 3 \text{ GeV}$ .

**Relic Density** – The dark sector can be in thermal bath through the decay and inverse decay of  $F$  to neutrino and photon. This requires the decay rate of  $F$ ,  $\Gamma \sim g_{F\nu A}^2 m_F^3 / (8\pi)$  to be larger than the Hubble constant,  $H \propto T^2/M_{\text{Pl}}$  where  $M_{\text{Pl}}$  is the Planck mass. By taking the freeze-out temperature  $T \sim m_\chi/25 \sim m_F/25$ , we need  $g_{F\nu A} \gtrsim 0.2/\sqrt{M_{\text{Pl}}m_F} \sim (10^{-12} \sim 10^{-10}) \text{ GeV}^{-1}$  as a function of  $m_F$ . Since  $g_{F\nu A}$  is a free parameter with no additional constraint, the requirement can be easily satisfied. Further, the DM particle  $\chi$  can also be in thermal equilibrium via the annihilation processes  $\chi\bar{\chi} \leftrightarrow F\bar{F}$ . For simplicity, we consider symmetric DM with vanishing chemical potential.

With the same mass difference  $\Delta_{F\chi}$  and self-scattering cross section  $\langle\sigma_T v\rangle$ , the allowed annihilation strength  $\langle\sigma v\rangle$  and DM mass  $m_\chi$  for generating the correct relic density  $\Omega_{\text{CDM}} = 0.12$  through freeze-out is shown as black line in Fig. 4. Both  $\chi\bar{\chi} \rightarrow F\bar{F}$  and  $\chi\bar{\chi} \rightarrow \phi\phi$  can happen in the early Universe to determine the DM relic density. With fixed DM self-scattering cross section  $\langle\sigma_T v\rangle/m_\chi = 1.5 (\text{cm}^2/\text{g}) \times (\text{km/s})$ , the coupling  $g_{\chi\phi}$  between  $\chi$  and  $\phi$  increases with the DM mass  $m_\chi$ . Being modulated by the same coupling, the cross section of  $\chi\bar{\chi} \rightarrow \phi\phi$  also increases with  $m_\chi$ . In other words, the

DM freeze-out is dominated by the second annihilation channel for heavy DM and the first channel should have decreasing cross section in order to obtain the correct relic density. At some point, no parameter space is left for the first channel which means the involved coupling  $g_{F\phi}$  should vanish. This explains why the black curve suddenly drops to zero.

We can see that the constraint from FermiLAT is consistent with the one from the DM relic density for  $m_\chi = 6.6 \text{ GeV}$ . However, this is not claiming that the forbidden DM has already been established by FermiLAT. More realistic analysis by the experimental collaboration is necessary which should give much more stringent bounds on  $\langle\sigma v\rangle$ .

The massive mediator  $\phi$  can decay into two neutrinos through loop correction with the massive fermion  $F$  in the triangle diagram. Taking the typical values  $g_{F\nu A} = 10^{-3} \text{ GeV}^{-1}$  and  $g_{F\phi} = 10^{-3}$ , the predicted rate  $\Gamma_\phi \simeq g_{F\phi}^2 g_{F\nu A}^4 m_F^4 m_\phi / 48\pi^3$  indicates that the mediator can decay within  $10^{-5} \text{ s}$  and hence does not contribute to the relic density. However, a light mediator with mass  $m_\phi \lesssim 1 \text{ MeV}$  can cause extra relativistic degrees of freedom. The grey band in Fig. 4 shows the parameter region constrained by BBN. Although the two-photon final state is also kinematically allowed, it is forbidden by the Landau-Yang theorem [76, 77] since  $\phi$  is a vector boson.

**Conclusion and Discussion** – We propose using SMBH as a natural accelerator to reactivate the forbidden DM to allow them to annihilate into heavier partners. The subsequent decay into  $\gamma$  photons can leave unique signature for astrophysical observation, such as those at Fermi-LAT. Two important features can be identified. First, the photon energy is mainly determined by the DM mass and its spectrum has a peak. Second, such a signal is always associated with SMBH instead of random distribution. If the angular resolution is good enough, more geometrical features can be identified.

### Acknowledgements

The authors would like to thank Xun Chen, Yu-Chen Wang, and Hai-Bo Yu for useful discussions. This work is supported by the National Natural Science Foundation of China (12375101, 12375088, 12090060, and 12090064), the Shanghai Pujiang Program (20PJ1407800), and the Double First Class start-up fund (WF220442604). XGH was also supported in part by the MOST (Grant No. MOST 106- 2112-M-002- 003-MY3 ). SFG is also an affiliate member of Kavli IPMU, University of Tokyo.

\* Corresponding Author: [chengyu@sjtu.edu.cn](mailto:chengyu@sjtu.edu.cn)

† Corresponding Author: [gesf@sjtu.edu.cn](mailto:gesf@sjtu.edu.cn)

<sup>†</sup> Electronic address: [hexg@sjtu.edu.cn](mailto:hexg@sjtu.edu.cn)

<sup>§</sup> Electronic address: [shengjie04@sjtu.edu.cn](mailto:shengjie04@sjtu.edu.cn)

- [1] A. Arbey and F. Mahmoudi, “*Dark matter and the early Universe: a review*,” *Prog. Part. Nucl. Phys.* **119**, 103865 (2021) [[arXiv:2104.11488](https://arxiv.org/abs/2104.11488)] [hep-ph].
- [2] B. L. Young, “*A survey of dark matter and related topics in cosmology*,” *Front. Phys. (Beijing)* **12**, no.2, 121201 (2017)
- [3] B. W. Lee and S. Weinberg, “*Cosmological Lower Bound on Heavy Neutrino Masses*,” *Phys. Rev. Lett.* **39**, 165-168 (1977)
- [4] L. J. Hall, K. Jedamzik, J. March-Russell and S. M. West, “*Freeze-In Production of FIMP Dark Matter*,” *JHEP* **03**, 080 (2010) [[arXiv:0911.1120](https://arxiv.org/abs/0911.1120)] [hep-ph].
- [5] M. Garny, J. Heisig, B. Lülz and S. Vogl, “*Coannihilation without chemical equilibrium*,” *Phys. Rev. D* **96**, no.10, 103521 (2017) [[arXiv:1705.09292](https://arxiv.org/abs/1705.09292)] [hep-ph].
- [6] R. T. D’Agnolo, C. Mondino, J. T. Ruderman and P. J. Wang, “*Exponentially Light Dark Matter from Coannihilation*,” *JHEP* **08**, 079 (2018) [[arXiv:1803.02901](https://arxiv.org/abs/1803.02901)] [hep-ph].
- [7] S. Mizuta and M. Yamaguchi, “*Coannihilation effects and relic abundance of Higgsino dominant LSP(s)*,” *Phys. Lett. B* **298**, 120-126 (1993) [[arXiv:hep-ph/9208251](https://arxiv.org/abs/hep-ph/9208251)] [hep-ph].
- [8] F. D’Eramo and J. Thaler, “*Semi-annihilation of Dark Matter*,” *JHEP* **06**, 109 (2010) [[arXiv:1003.5912](https://arxiv.org/abs/1003.5912)] [hep-ph].
- [9] G. Bélanger, K. Kannike, A. Pukhov and M. Raidal, “*Minimal semi-annihilating  $\mathbb{Z}_N$  scalar dark matter*,” *JCAP* **06**, 021 (2014) [[arXiv:1403.4960](https://arxiv.org/abs/1403.4960)] [hep-ph].
- [10] Y. Cai and A. P. Spray, “*Fermionic Semi-Annihilating Dark Matter*,” *JHEP* **01**, 087 (2016) [[arXiv:1509.08481](https://arxiv.org/abs/1509.08481)] [hep-ph].
- [11] P. Bandyopadhyay, D. Choudhury and D. Sachdeva, “*Semi-Annihilation of Fermionic Dark Matter*,” [[arXiv:2206.05811](https://arxiv.org/abs/2206.05811)] [hep-ph].
- [12] U. K. Dey, T. N. Maity and T. S. Ray, “*Light Dark Matter through Assisted Annihilation*,” *JCAP* **03**, 045 (2017) [[arXiv:1612.09074](https://arxiv.org/abs/1612.09074)] [hep-ph].
- [13] K. Hashino, J. Liu, X. P. Wang and K. P. Xie, “*Dark matter transient annihilations in the early Universe*,” *Phys. Rev. D* **105**, no.5, 055009 (2022) [[arXiv:2109.07479](https://arxiv.org/abs/2109.07479)] [hep-ph].
- [14] T. Bringmann, P. F. Depta, M. Hufnagel, J. T. Ruderman and K. Schmidt-Hoberg, “*Dark Matter from Exponential Growth*,” *Phys. Rev. Lett.* **127**, no.19, 19 (2021) [[arXiv:2103.16572](https://arxiv.org/abs/2103.16572)] [hep-ph].
- [15] Chuan-Yang Xing and S. H. Zhu, “*Dark Matter Freeze-Out via Catalyzed Annihilation*,” *Phys. Rev. Lett.* **127**, no.6, 061101 (2021) [[arXiv:2102.02447](https://arxiv.org/abs/2102.02447)] [hep-ph].
- [16] L. Puetter, J. T. Ruderman, E. Salvioni and B. Shakya, “*Bouncing Dark Matter*,” [[arXiv:2208.08453](https://arxiv.org/abs/2208.08453)] [hep-ph].
- [17] S. Dodelson and L. M. Widrow, “*Sterile-neutrinos as dark matter*,” *Phys. Rev. Lett.* **72**, 17-20 (1994) [[arXiv:hep-ph/9303287](https://arxiv.org/abs/hep-ph/9303287)] [hep-ph].
- [18] M. Pospelov, A. Ritz and M. B. Voloshin, “*Secluded WIMP Dark Matter*,” *Phys. Lett. B* **662**, 53-61 (2008) [[arXiv:0711.4866](https://arxiv.org/abs/0711.4866)] [hep-ph].
- [19] Y. Hochberg, E. Kuflik, T. Volansky and J. G. Wacker, “*Mechanism for Thermal Relic Dark Matter of Strongly Interacting Massive Particles*,” *Phys. Rev. Lett.* **113**, 171301 (2014) [[arXiv:1402.5143](https://arxiv.org/abs/1402.5143)] [hep-ph].
- [20] Y. Hochberg, E. Kuflik, H. Murayama, T. Volansky and J. G. Wacker, “*Model for Thermal Relic Dark Matter of Strongly Interacting Massive Particles*,” *Phys. Rev. Lett.* **115**, no.2, 021301 (2015) [[arXiv:1411.3727](https://arxiv.org/abs/1411.3727)] [hep-ph].
- [21] N. Bernal, X. Chu and J. Pradler, “*Simply split strongly interacting massive particles*,” *Phys. Rev. D* **95**, no.11, 115023 (2017) [[arXiv:1702.04906](https://arxiv.org/abs/1702.04906)] [hep-ph].
- [22] R. T. D’Agnolo and A. Hook, “*Selfish Dark Matter*,” *Phys. Rev. D* **91**, no.11, 115020 (2015) [[arXiv:1504.00361](https://arxiv.org/abs/1504.00361)] [hep-ph].
- [23] K. Griest and D. Seckel, “*Three exceptions in the calculation of relic abundances*,” *Phys. Rev. D* **43**, 3191-3203 (1991)
- [24] R. T. D’Agnolo and J. T. Ruderman, “*Light Dark Matter from Forbidden Channels*,” *Phys. Rev. Lett.* **115**, no.6, 061301 (2015) [[arXiv:1505.07107](https://arxiv.org/abs/1505.07107)] [hep-ph].
- [25] J. Kopp, J. Liu, T. R. Slatyer, X. P. Wang and W. Xue, “*Impeded Dark Matter*,” *JHEP* **12**, 033 (2016) [[arXiv:1609.02147](https://arxiv.org/abs/1609.02147)] [hep-ph].
- [26] A. Delgado, A. Martin and N. Raj, “*Forbidden Dark Matter at the Weak Scale via the Top Portal*,” *Phys. Rev. D* **95**, no.3, 035002 (2017) [[arXiv:1608.05345](https://arxiv.org/abs/1608.05345)] [hep-ph].
- [27] R. T. D’Agnolo, D. Liu, J. T. Ruderman and P. J. Wang, “*Forbidden dark matter annihilations into Standard Model particles*,” *JHEP* **06**, 103 (2021) [[arXiv:2012.11766](https://arxiv.org/abs/2012.11766)] [hep-ph].
- [28] G. N. Wojcik and T. G. Rizzo, “*Forbidden scalar dark matter and dark Higgses*,” *JHEP* **04**, 033 (2022) [[arXiv:2109.07369](https://arxiv.org/abs/2109.07369)] [hep-ph].
- [29] J. M. Cline, H. Liu, T. Slatyer and W. Xue, “*Enabling Forbidden Dark Matter*,” *Phys. Rev. D* **96**, no.8, 083521 (2017) [[arXiv:1702.07716](https://arxiv.org/abs/1702.07716)] [hep-ph].
- [30] S. Tulin, Hai-Bo Yu and K. M. Zurek, “*Three Exceptions for Thermal Dark Matter with Enhanced Annihilation to  $\gamma\gamma$* ,” *Phys. Rev. D* **87**, no.3, 036011 (2013) [[arXiv:1208.0009](https://arxiv.org/abs/1208.0009)] [hep-ph].
- [31] C. B. Jackson, G. Servant, G. Shaughnessy, T. M. P. Tait and M. Taoso, “*Gamma-ray lines and One-Loop Continuum from s-channel Dark Matter Annihilations*,” *JCAP* **07**, 021 (2013) [[arXiv:1302.1802](https://arxiv.org/abs/1302.1802)] [hep-ph].
- [32] C. B. Jackson, G. Servant, G. Shaughnessy, T. M. P. Tait and M. Taoso, “*Gamma Rays from Top-Mediated Dark Matter Annihilations*,” *JCAP* **07**, 006 (2013) [[arXiv:1303.4717](https://arxiv.org/abs/1303.4717)] [hep-ph].
- [33] P. Gondolo and J. Silk, “*Dark matter annihilation at the galactic center*,” *Phys. Rev. Lett.* **83**, 1719-1722 (1999) [[arXiv:astro-ph/9906391](https://arxiv.org/abs/astro-ph/9906391)] [astro-ph].
- [34] D. Merritt, “*Evolution of the dark matter distribution at the galactic center*,” *Phys. Rev. Lett.* **92**, 201304 (2004) [[arXiv:astro-ph/0311594](https://arxiv.org/abs/astro-ph/0311594)] [astro-ph].
- [35] O. Y. Gnedin and J. R. Primack, “*Dark Matter Profile in the Galactic Center*,” *Phys. Rev. Lett.* **93**, 061302 (2004) [[arXiv:astro-ph/0308385](https://arxiv.org/abs/astro-ph/0308385)] [astro-ph].
- [36] M. Regis and P. Ullio, “*Multi-wavelength signals of dark matter annihilations at the Galactic center*,” *Phys. Rev. D* **78**, 043505 (2008) [[arXiv:0802.0234](https://arxiv.org/abs/0802.0234)] [hep-ph].
- [37] B. D. Fields, S. L. Shapiro and J. Shelton, “*Galactic Center Gamma-Ray Excess from Dark Matter Annihilation: Is There A Black Hole Spike?*,” *Phys. Rev. Lett.* **113**, 151302 (2014) [[arXiv:1406.4856](https://arxiv.org/abs/1406.4856)] [astro-ph.HE].
- [38] P. Sandick, K. Sinha and T. Yamamoto, “*Black Holes, Dark Matter Spikes, and Constraints on Simplified Models with t-Channel Mediators*,” *Phys. Rev. D* **98**, no.3, 035004 (2018) [[arXiv:1701.00067](https://arxiv.org/abs/1701.00067)] [hep-ph].
- [39] J. Shelton, S. L. Shapiro and B. D. Fields, “*Black hole*

- window into  $p$ -wave dark matter annihilation,” *Phys. Rev. Lett.* **115**, no.23, 231302 (2015) [arXiv:1506.04143 [astro-ph.HE]].
- [40] C. Johnson, R. Caputo, C. Karwin, S. Murgia, S. Ritz and J. Shelton, “Search for gamma-ray emission from  $p$ -wave dark matter annihilation in the Galactic Center,” *Phys. Rev. D* **99**, no.10, 103007 (2019) [arXiv:1904.06261 [astro-ph.HE]].
- [41] B. T. Chiang, S. L. Shapiro and J. Shelton, “Faint dark matter annihilation signals and the Milky Way’s super-massive black hole,” *Phys. Rev. D* **102**, no.2, 023030 (2020) [arXiv:1912.09446 [hep-ph]].
- [42] G. W. Yuan, Z. F. Chen, Z. Q. Shen, W. Q. Guo, Ran Ding, X. Huang and Qiang Yuan, “Constraints on dark matter annihilation from the Event Horizon Telescope observations of M87,” *JHEP* **04**, 018 (2022) [arXiv:2106.05901 [hep-ph]].
- [43] Z. Q. Xia, Z. Q. Shen, X. Pan, L. Feng and Yi-Zhong Fan, “Investigating the dark matter minispikes with the gamma-ray signal from the halo of M31,” [arXiv:2108.09204 [astro-ph.HE]].
- [44] A. N. Baushev, “Dark matter annihilation in the gravitational field of a black hole,” *Int. J. Mod. Phys. D* **18**, 1195 (2009) [arXiv:0805.0124 [astro-ph]].
- [45] M. Banados, J. Silk and S. M. West, “Kerr Black Holes as Particle Accelerators to Arbitrarily High Energy,” *Phys. Rev. Lett.* **103**, 111102 (2009) [arXiv:0909.0169 [hep-ph]].
- [46] H. Abdallah *et al.* [HESS], “Search for  $\gamma$ -Ray Line Signals from Dark Matter Annihilations in the Inner Galactic Halo from 10 Years of Observations with H.E.S.S.,” *Phys. Rev. Lett.* **120**, no.20, 201101 (2018) [arXiv:1805.05741 [astro-ph.HE]].
- [47] V. Lefranc *et al.* [H.E.S.S.], “Dark matter search in the inner galactic center halo with H.E.S.S.,” [arXiv:1608.08453 [astro-ph.HE]].
- [48] A. Abramowski *et al.* [H.E.S.S.], “Search for a Dark Matter annihilation signal from the Galactic Center halo with H.E.S.S.,” *Phys. Rev. Lett.* **106**, 161301 (2011) [arXiv:1103.3266 [astro-ph.HE]].
- [49] G. Alvarez and Hai-Bo Yu, “Density spikes near black holes in self-interacting dark matter halos and indirect detection constraints,” *Phys. Rev. D* **104**, no.4, 043013 (2021) [arXiv:2012.15050 [hep-ph]].
- [50] T. Harada and M. Kimura, “Black holes as particle accelerators: a brief review,” *Class. Quant. Grav.* **31**, 243001 (2014) [arXiv:1409.7502 [gr-qc]].
- [51] F. Jüttner, “Das Maxwellsche Gesetz der Geschwindigkeitsverteilung in der Relativtheorie,” *Ann. Phys.* **339**, 856(1911).
- [52] S. R. De Groot, W. A. Van Leeuwen and C. G. Van Weert, “Relativistic Kinetic Theory. Principles and Applications, 1980, ISBN 13: 9780444854537.”
- [53] M. Cannoni, “Relativistic  $\langle\sigma v_{\text{rel}}\rangle$  in the calculation of relics abundances: a closer look,” *Phys. Rev. D* **89**, no.10, 103533 (2014) [arXiv:1311.4494 [astro-ph.CO]].
- [54] M. Cannoni, “Relativistic and nonrelativistic annihilation of dark matter: a sanity check using an effective field theory approach,” *Eur. Phys. J. C* **76**, no.3, 137 (2016) [arXiv:1506.07475 [hep-ph]].
- [55] M. Kaplinghat, S. Tulin and Hai-Bo Yu, “Dark Matter Halos as Particle Colliders: Unified Solution to Small-Scale Structure Puzzles from Dwarfs to Clusters,” *Phys. Rev. Lett.* **116**, no.4, 041302 (2016) [arXiv:1508.03339 [astro-ph.CO]].
- [56] J. F. Navarro, C. S. Frenk and S. D. M. White, “The Structure of cold dark matter halos,” *Astrophys. J.* **462**, 563-575 (1996) [arXiv:astro-ph/9508025 [astro-ph]].
- [57] K. N. Abazajian, S. Horiuchi, M. Kaplinghat, R. E. Keeley and O. Macias, “Strong constraints on thermal relic dark matter from Fermi-LAT observations of the Galactic Center,” *Phys. Rev. D* **102**, no.4, 043012 (2020) [arXiv:2003.10416 [hep-ph]].
- [58] M. Kaplinghat, R. E. Keeley, T. Linden and Hai-Bo Yu, “Tying Dark Matter to Baryons with Self-interactions,” *Phys. Rev. Lett.* **113**, 021302 (2014) [arXiv:1311.6524 [astro-ph.CO]].
- [59] J. L. Feng, M. Kaplinghat and Hai-Bo Yu, “Halo Shape and Relic Density Exclusions of Sommerfeld-Enhanced Dark Matter Explanations of Cosmic Ray Excesses,” *Phys. Rev. Lett.* **104**, 151301 (2010) [arXiv:0911.0422 [hep-ph]].
- [60] S. Tulin, Hai-Bo Yu and K. M. Zurek, “Beyond Collisionless Dark Matter: Particle Physics Dynamics for Dark Matter Halo Structure,” *Phys. Rev. D* **87**, no.11, 115007 (2013) [arXiv:1302.3898 [hep-ph]].
- [61] K. Schutz and T. R. Slatyer, “Self-Scattering for Dark Matter with an Excited State,” *JCAP* **01**, 021 (2015) [arXiv:1409.2867 [hep-ph]].
- [62] S. Tulin and Hai-Bo Yu, “Dark Matter Self-interactions and Small Scale Structure,” *Phys. Rept.* **730**, 1-57 (2018) [arXiv:1705.02358 [hep-ph]].
- [63] S. L. Shapiro and V. Paschalidis, “Self-interacting dark matter cusps around massive black holes,” *Phys. Rev. D* **89**, no.2, 023506 (2014) [arXiv:1402.0005 [astro-ph.CO]].
- [64] L. Sadeghian, F. Ferrer and C. M. Will, “Dark matter distributions around massive black holes: A general relativistic analysis,” *Phys. Rev. D* **88**, no.6, 063522 (2013) [arXiv:1305.2619 [astro-ph.GA]].
- [65] J. Hisano, S. Matsumoto and M. M. Nojiri, “Unitarity and higher order corrections in neutralino dark matter annihilation into two photons,” *Phys. Rev. D* **67**, 075014 (2003) [arXiv:hep-ph/0212022 [hep-ph]].
- [66] J. Hisano, S. Matsumoto and M. M. Nojiri, “Explosive dark matter annihilation,” *Phys. Rev. Lett.* **92**, 031303 (2004) [arXiv:hep-ph/0307216 [hep-ph]].
- [67] J. Hisano, S. Matsumoto, M. Nagai, O. Saito and M. Senami, “Non-perturbative effect on thermal relic abundance of dark matter,” *Phys. Lett. B* **646**, 34-38 (2007) [arXiv:hep-ph/0610249 [hep-ph]].
- [68] N. Arkani-Hamed, D. P. Finkbeiner, T. R. Slatyer and N. Weiner, “A Theory of Dark Matter,” *Phys. Rev. D* **79**, 015014 (2009) [arXiv:0810.0713 [hep-ph]].
- [69] A. Ibarra, S. Lopez Gehler and M. Pato, “Dark matter constraints from box-shaped gamma-ray features,” *JCAP* **07**, 043 (2012) [arXiv:1205.0007 [hep-ph]].
- [70] A. Ibarra, H. M. Lee, S. López Gehler, W. I. Park and M. Pato, “Gamma-ray boxes from axion-mediated dark matter,” *JCAP* **05**, 016 (2013) [arXiv:1303.6632 [hep-ph]].
- [71] W. B. Atwood *et al.* [Fermi-LAT], “The Large Area Telescope on the Fermi Gamma-ray Space Telescope Mission,” *Astrophys. J.* **697**, 1071-1102 (2009) [arXiv:0902.1089 [astro-ph.IM]].
- [72] A. Albert *et al.* [Fermi-LAT and DES], “Searching for Dark Matter Annihilation in Recently Discovered Milky Way Satellites with Fermi-LAT,” *Astrophys. J.* **834**, no.2, 110 (2017) [arXiv:1611.03184 [astro-ph.HE]].

- [73] S. Abdollahi *et al.* [Fermi-LAT], “*Fermi Large Area Telescope Fourth Source Catalog*,” [Astrophys. J. Suppl. \*\*247\*\*, no.1, 33 \(2020\) \[arXiv:1902.10045 \[astro-ph.HE\]\]](#).
- [74] J. Ballet *et al.* [Fermi-LAT], “*Fermi Large Area Telescope Fourth Source Catalog Data Release 2*,” [\[arXiv:2005.11208 \[astro-ph.HE\]\]](#).
- [75] F. Cafardo *et al.* [Fermi-LAT], “*Fermi-LAT Observations of Sagittarius A\*: Imaging Analysis*,” [Astrophys. J. \*\*918\*\*, no.1, 30 \(2021\) \[arXiv:2107.00756 \[astro-ph.HE\]\]](#).
- [76] L. D. Landau, “*On the angular momentum of a system of two photons*,” [Dokl. Akad. Nauk SSSR \*\*60\*\*, no.2, 207-209 \(1948\)](#)
- [77] C. N. Yang, “*Selection Rules for the Dematerialization of a Particle Into Two Photons*,” [Phys. Rev. \*\*77\*\*, 242-245 \(1950\)](#)